Supporting Information

Dual-emission 3D supramolecular framework hydrogel beads: highly selective detection of antibiotics and mechanism research

Ke Zhu, Ruiqing Fan* Jian Zhang, Xin Jiang, Wenwen Jia, Bowen Wang, Haoyang Lu, Jingkun Wu, Ping Wang and Yulin Yang*

K. Zhu, Prof. R. Fan, J. Zhang, X. Jiang, W. Jia, B. Wang, H. Lu, J. Wu, P. Wang and Prof. Y. Yang
MIIT Key Laboratory of Critical Materials Technology for New Energy Conversion and Storage, School of Chemistry and Chemical Engineering, Harbin Institute of Technology, Harbin 150001, P. R. China
E-mail: fanruiqing@hit.edu.cn and ylyang@hit.edu.cn

Materials and Methods

All the other materials were commercially available reagents of analytical grade. Single-crystal X-ray diffraction (SC-XRD) data of **Cu-cboa** and **Cu-atda** were obtained by Rigaku SCX-mini diffractometer with graphite monochromatic Mo-Kα radiation (λ = 0.71073 Å). Powder X-ray diffraction (PXRD) pattern was obtained using Cu Kα radiation with Shimadzu XRD-6000 X-ray diffractometer. Simulation of PXRD pattern was performed by single crystal data and diffraction crystal module of Mercury program. Thermogravimetric analysis (TGA) was carried out on ZRY-2P thermogravimetric analyzer from 40 to 700 °C with a heating rate of 10 °C/min under air atmosphere. Scan electron microscope (SEM) image was recorded by Rili SU 8000HSD Series Hitachi New Generation Cold Field Emission. The emission properties were recorded with Edinburgh FLS 920 fluorescence spectrometer equipped with a Peltier-cooled Hamamatsu R928 photomultiplier tube. An Edinburgh Xe900 450 W xenon arc lamp was used as an exciting light source.

Single-Crystal X-Ray Crystal Structure Determination

The X-ray diffraction data taken at room temperature for **Cu-cboa** and **Cu-atda** were collected on a Rigaku R-AXIS RAPID IP diffractometer equipped with graphite-monochromated Mo Kα radiation (λ = 0. 71073 Å). The structure of **Cu-cboa** and **Cu-atda** were solved by direct methods and refined on F^2 by the full-matrix least squares using the SHELXTL-97 crystallographic software. Anisotropic thermal parameters are refined to all of the non-hydrogen atoms. The hydrogen atoms were held in calculated ideal positions on carbon atoms and nitrogen atoms in ligands. The chemical formulas were determined by the combination of single crystal data, TGA results and elemental analysis. The CCDC 2101623 and 2101553 contains the crystallographic data **Cu-cboa**

and **Cu-atda** of this paper. These data can be obtained free of charge at www.ccdc.cam.ac.uk/ deposit. Crystal structure data and details of the data collection and the structure refinement are listed as Table S1and S2.

DFT calculations detail

9A/Cu-atda and antibiotic molecules are modeled by referring the previous literature, DFT and TD-DFT calculations were performed with Gaussian 09w. All molecular structure modeling were achieved by Gaussview 6.0. The B3LYP function was chosen to optimize the geometries and calculate triplet and singlet energy levels of antibiotic molecules. All Gaussian 09w calculations were conducted using 6-311g basis set for H, C, N, O, F and Cl atoms and Lanl2DZ effective core potentials for Cu atoms. Geometry optimizations of these models were converged to the S = 1 spin state. Finally, the global minimum was achieved for optimized.

■ EXPERIMENTAL SECTION

Sensing experiments

The **9A/Cu-atda@Eu^{3+}/SA** beads were immersed into different concentrations of antibiotics solutions (5 - 50 μM), and then take out it from the antibiotics solutions. Subsequently, the fluorescence intensity of the **9A/Cu-atda@Eu^{3+}/SA** were measured at an excitation wavelength of 330 nm. In order to verify the selectivity of **9A/Cu-atda@Eu^{3+}/SA** for FQ, NFT and NFZ, various common cations (such as, Na^+, Ca^{2+} etc.), anions (Cl^-, NO_2^- etc.), antibiotics were examined. The concentration of these substances were three times the concentration of FQ, NFT and NFZ (the concentration of FQ, NFT and NFZ solution was 1mM).

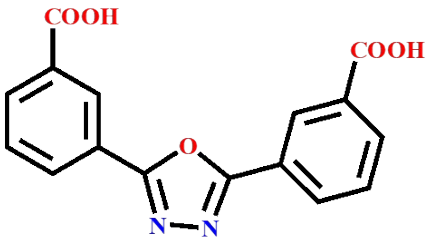

H_2cboa
2,5-bis(3-carboxylphenyl)-1,3,4-oxadiazole

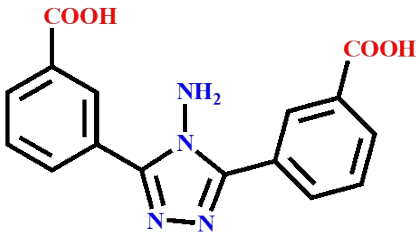

H_2adta
3,3'-(4-amino-1,2,4-triazol-3,5-diyl) dibenzoic acid

Fig. S1 The structural formula for the two ligands.

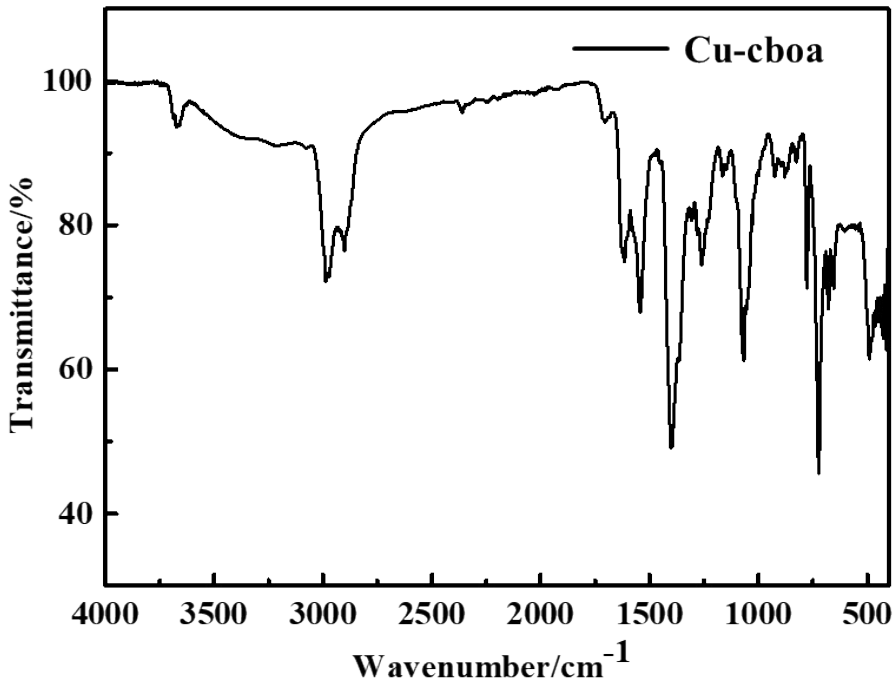

Fig. S2 FTIR spectra of **Cu-cboa**.

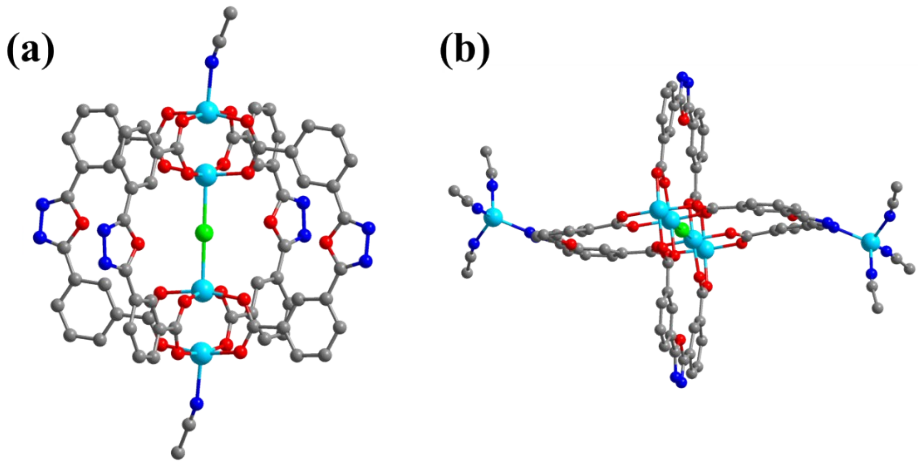

Fig. S3 (a) Unit 1**;** (b) Unit 2.

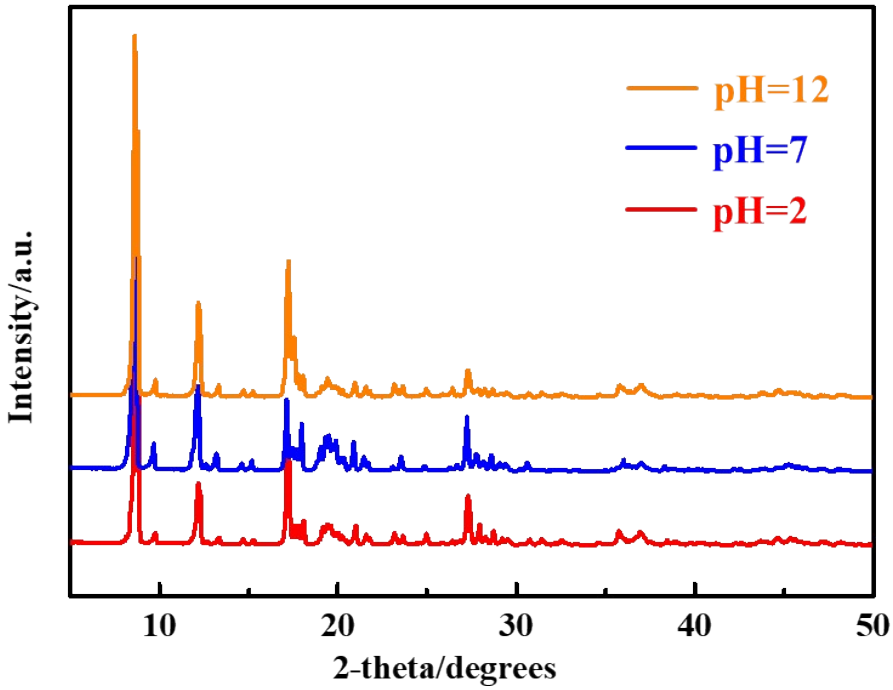

Fig. S4 PXRD patterns of **Cu-atda** under 24 h aqueous solution treatment of different pH values.

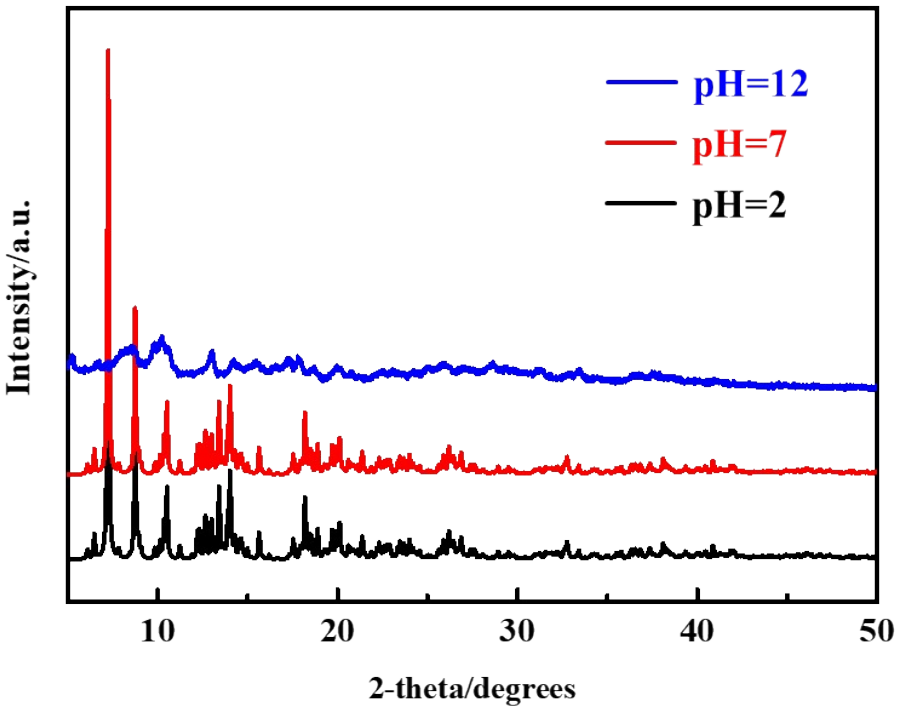

Fig. S5 PXRD patterns of **Cu-cboa** under 24 h aqueous solution treatment of different pH values.

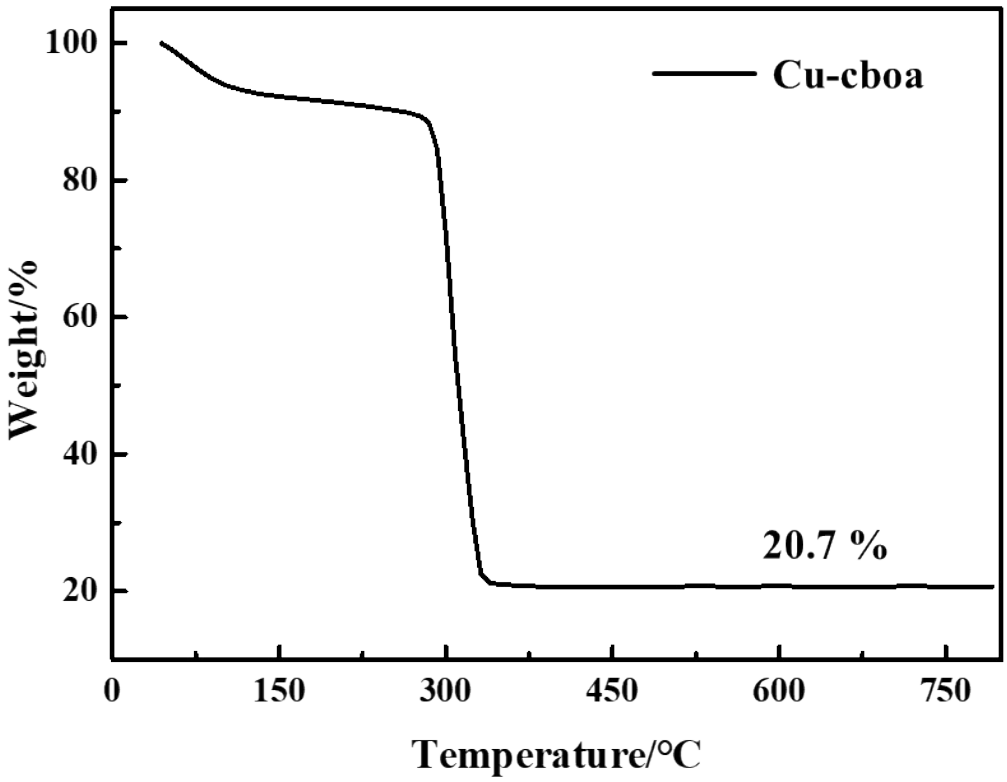

Fig. S6 The TG curves of **Cu-cboa**.

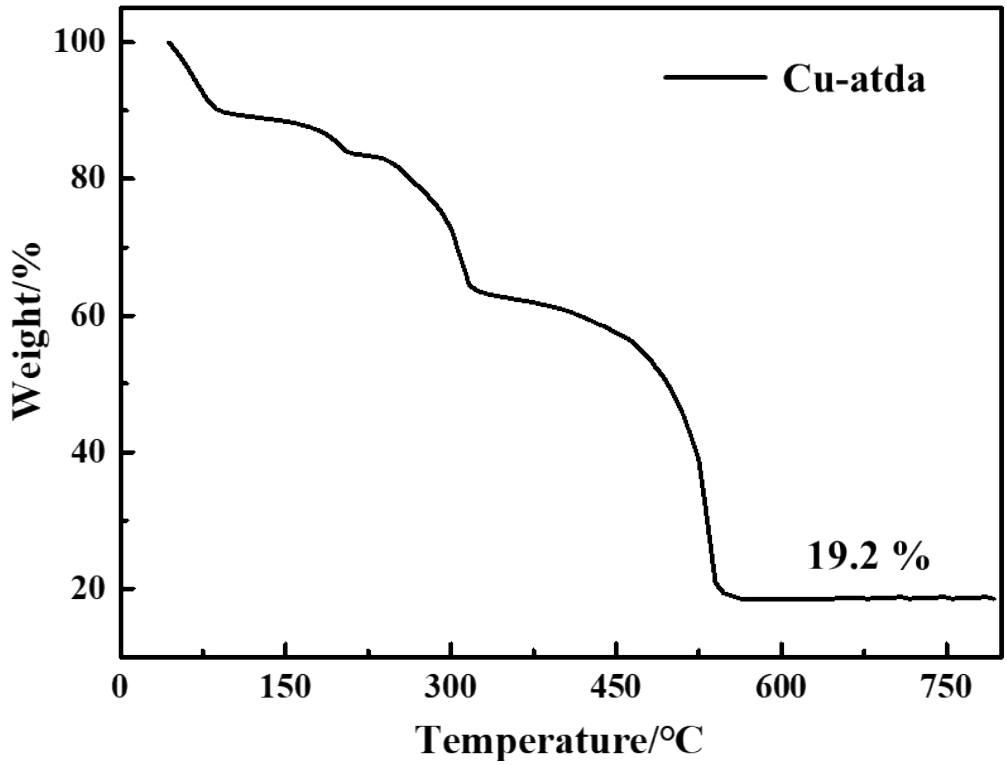

Fig. S7 The TG curves of **Cu-atda**.

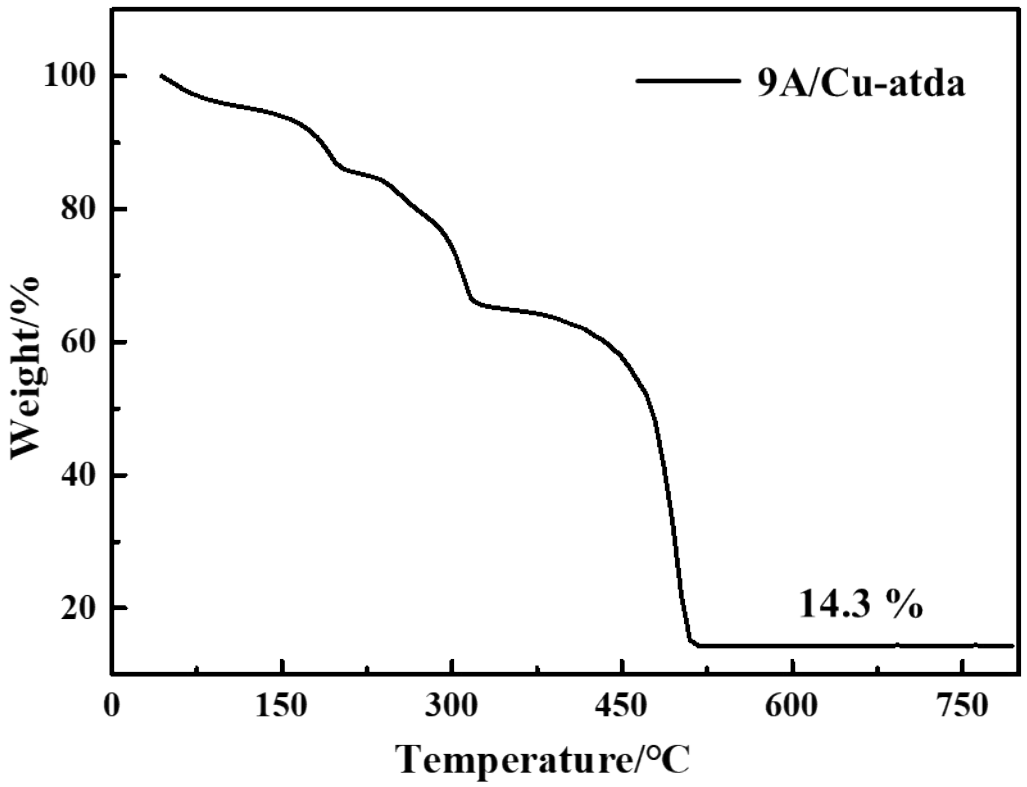

Fig. S8 The TG curves of **9A/Cu-atda**.

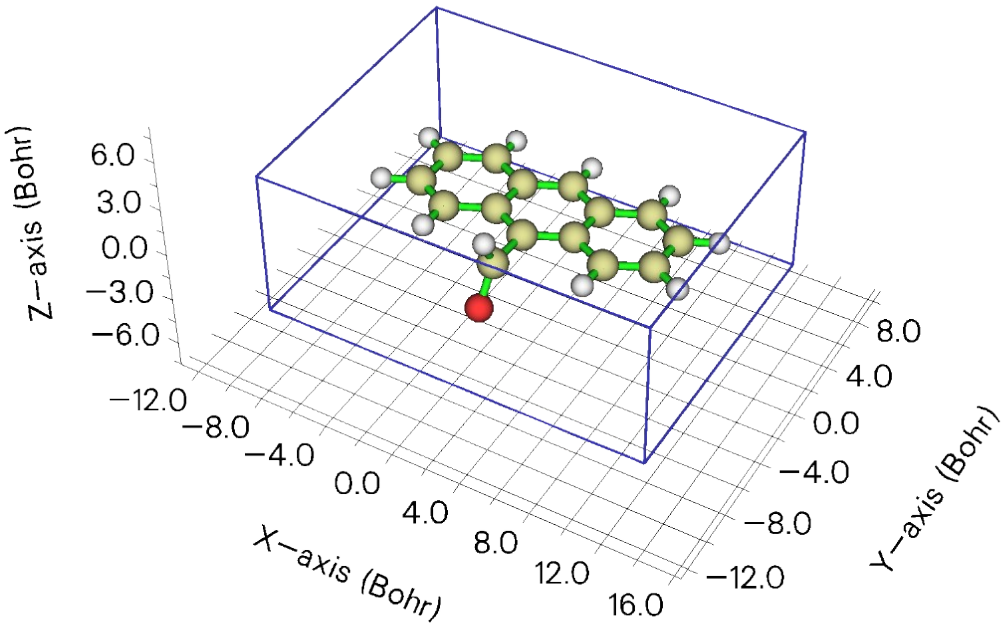

Fig. S9 The molecular size of 9A.

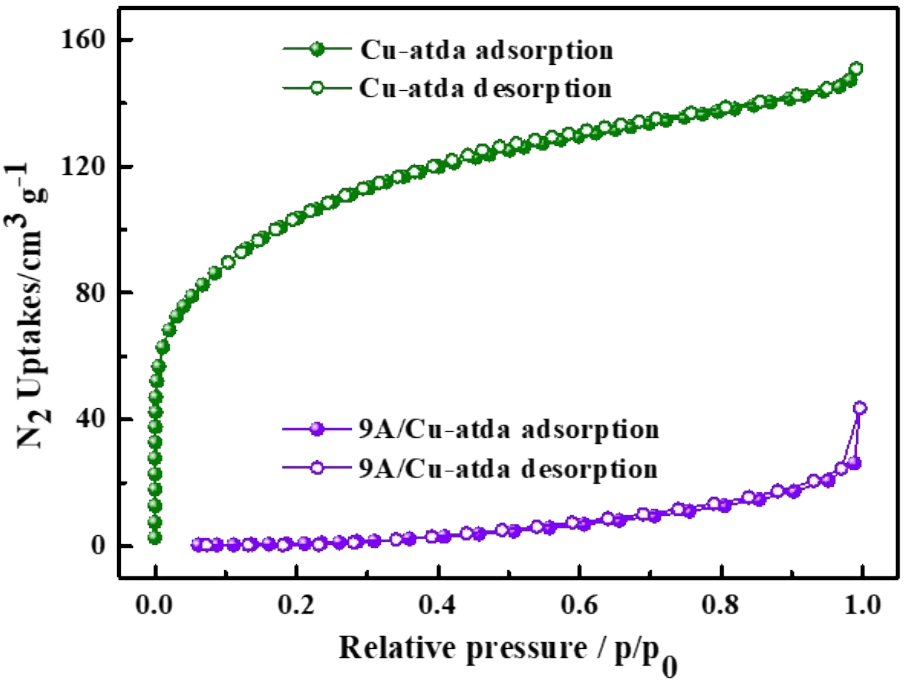

Fig. S10 N_2 adsorption and desorption isotherms of **Cu-atda**, **9A/Cu-atda**.

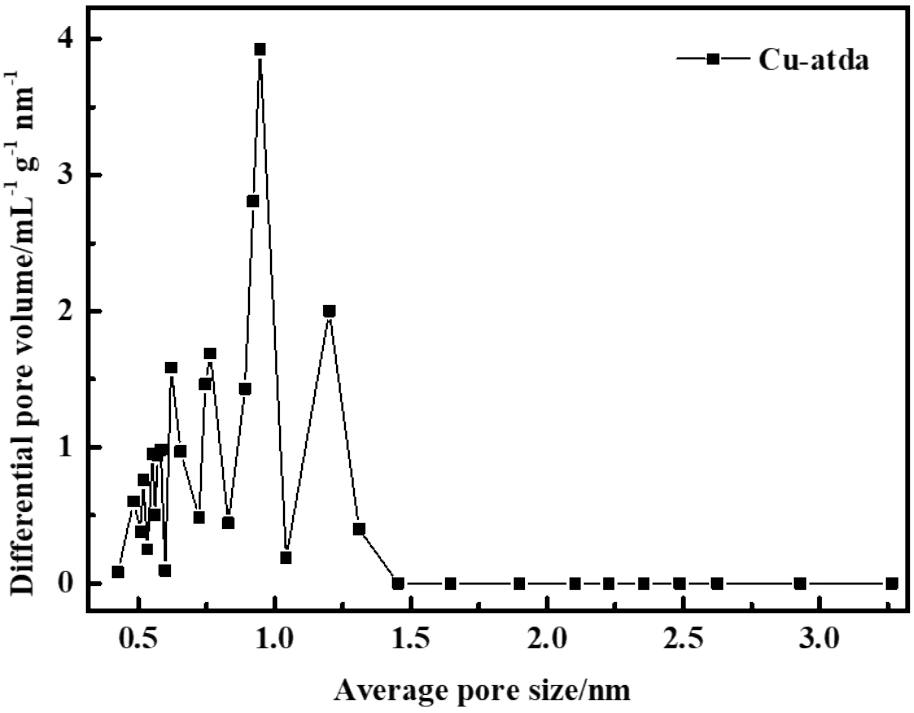

Fig. S11 the pore-size distribution curves of Cu-atda.

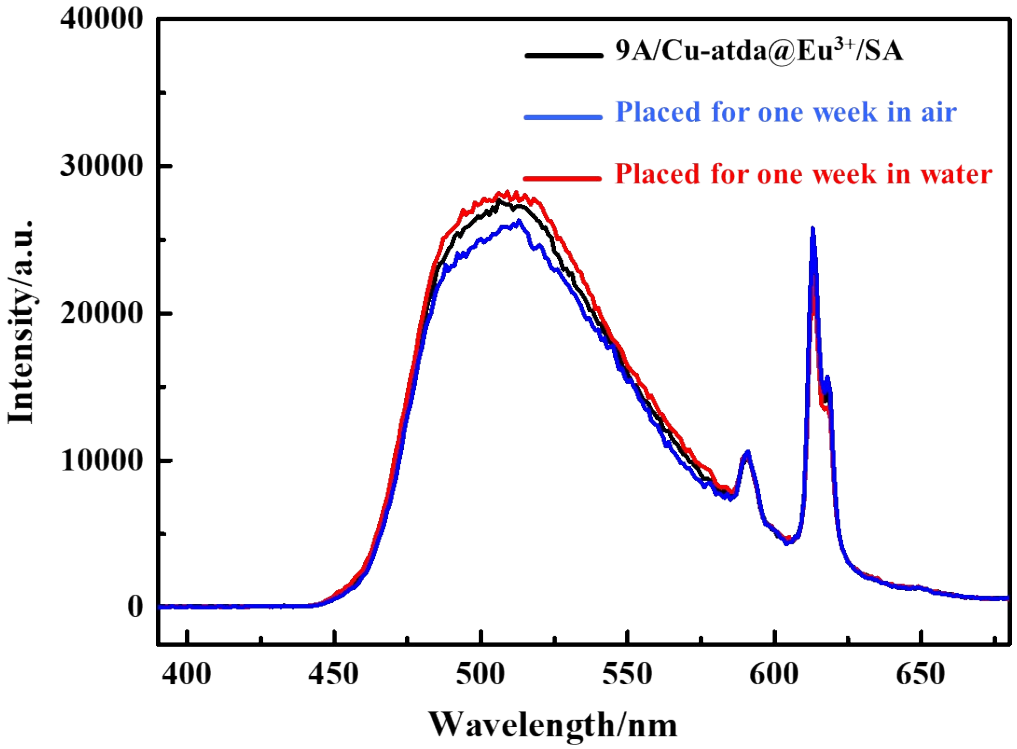

Fig. S12 the fluorescence stability of **9A/Cu-atda@Eu^{3+}/SA.**

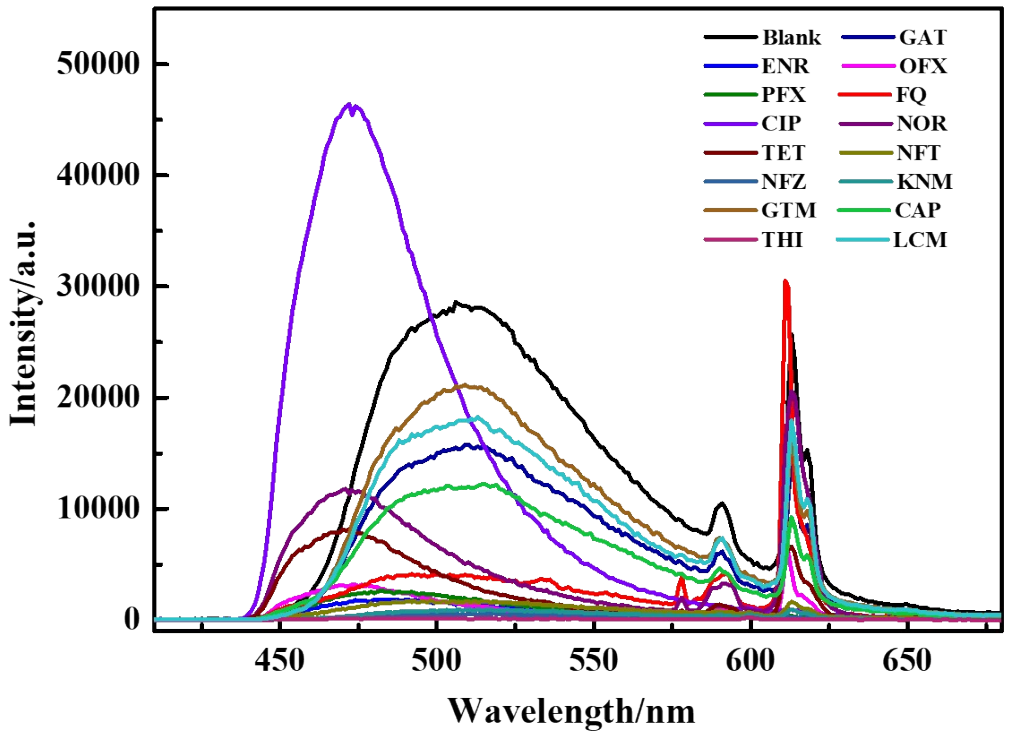

Fig. S13 The response of **9A/Cu-atda@Eu^{3+}/SA** to different substances.

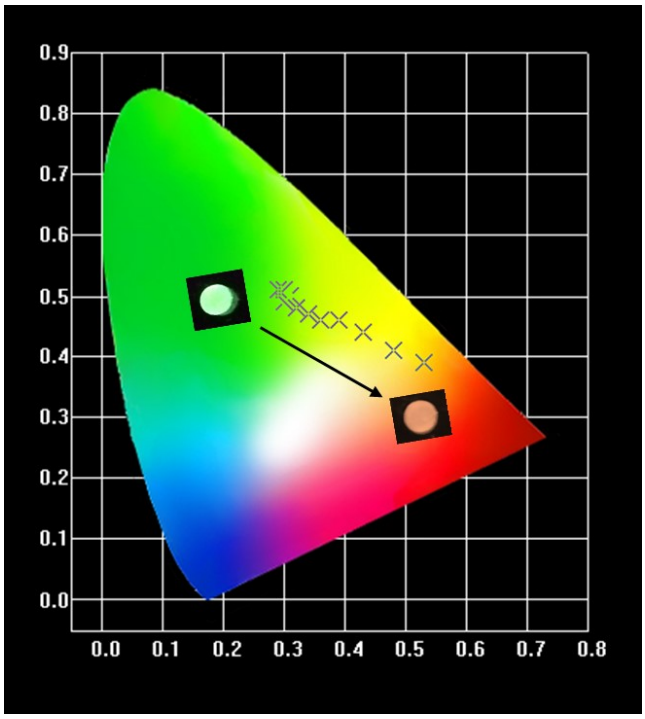

Fig. S14 CIE coordinates of **9A/Cu-adta@Eu^{3+}/SA** in different concentrations of FQ.

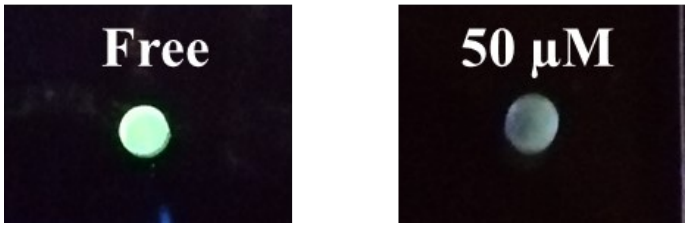

Fig. S15 Visual luminescent images of **9A/Cu-adta@Eu^{3+}/SA** beads in 50μM FQ under UV light.

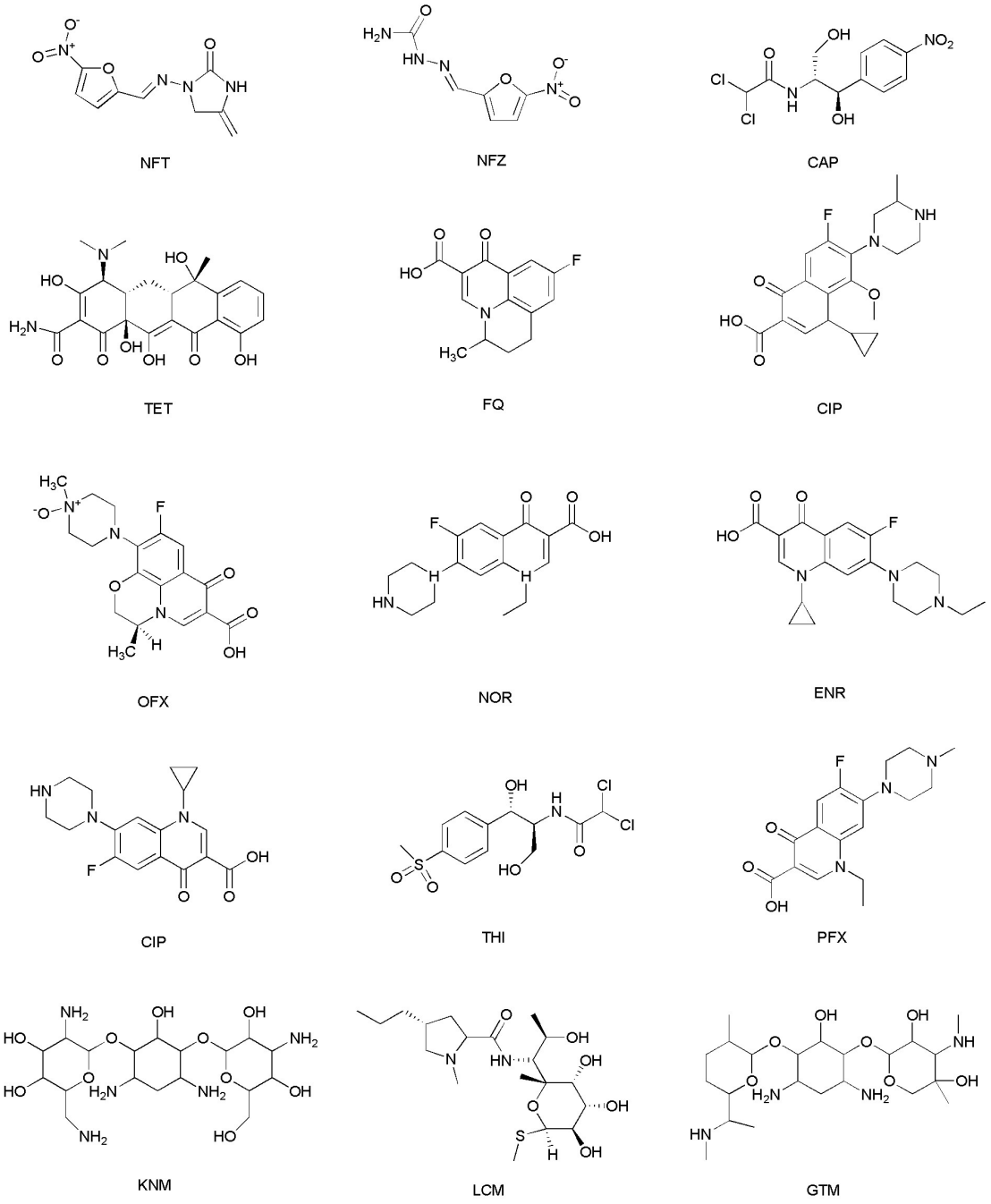

Fig. S16 Chemical structure of antibiotics.

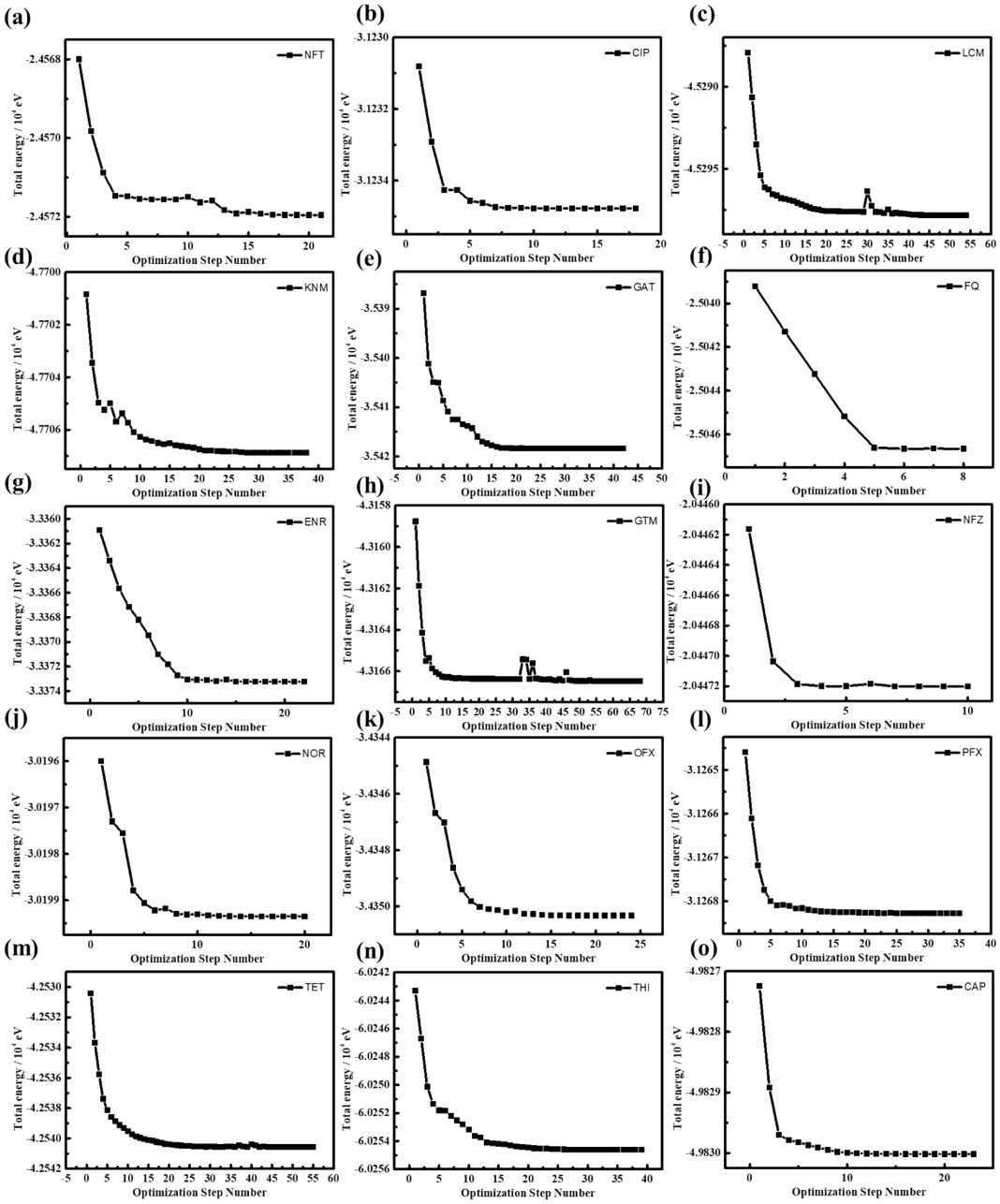

Fig. S17 The total energy and global minimum for optimized structures toward the 15 antibiotics.

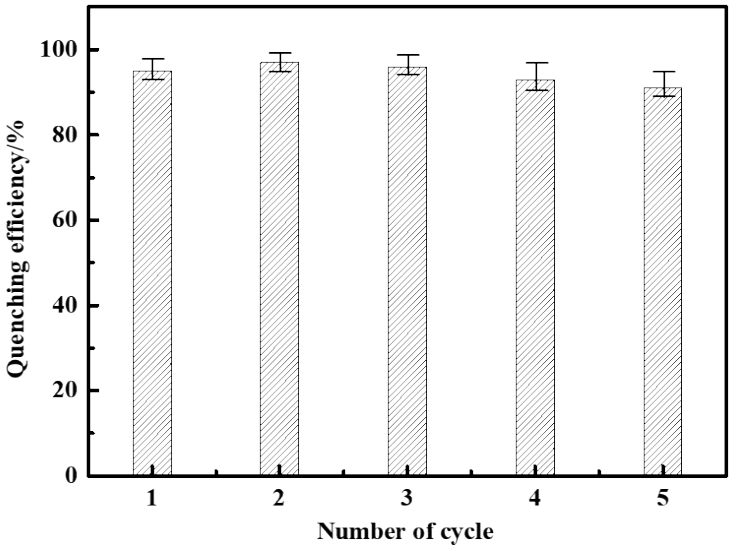

Fig. S18 Reusability of **9A/Cu-atda@Eu^{3+}/SA** beads for the detection of NFT (The used **9A/Cu-atda@Eu^{3+}/SA** beads was washed with ethanol and water).

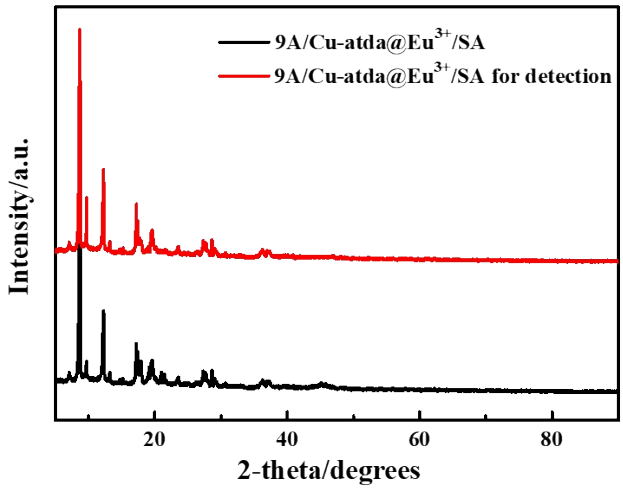

Fig. S19 PXRD patterns of **9A/Cu-atda@Eu^{3+}/SA** before and after detection**.**

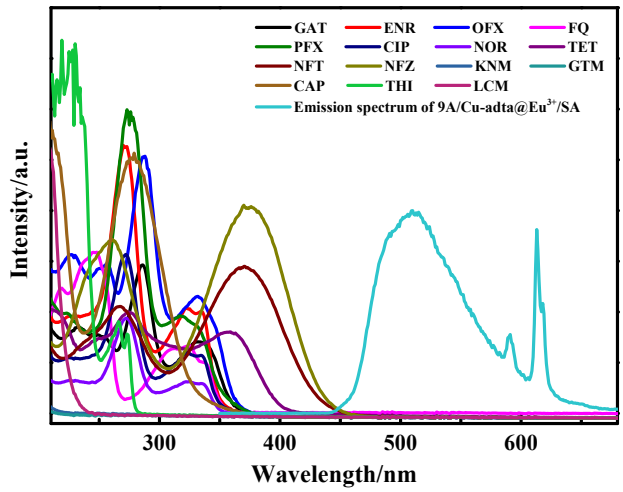

Fig. S20 Emission spectra of the **9A/Cu-atda@Eu^{3+}/SA** and the UV spectra of antibiotics.

Table S1. Crystal data and structure refinement parameters of **Cu-cboa**

Identification code	**Cu-cboa**
Empirical formula	$C_{72}H_{46}Cu_5IN_{11}O_{24}$
CCDC	2101623
Formula mass	1893.85
Crystal system	triclinic
Space group	P-1
a (Å)	13.8320(2)
b (Å)	14.5550(3)
c (Å)	20.1380(9)
α (˚)	84.923
β (˚)	80.195
γ (˚)	87.158
V (Å3)	3976.9
Z	2
Dc/(Mg m^{-3})	1.582
μ (Mo Kα)/mm^{-1}	1.784
F(000)	1890
θ range (°)	2.088 –24.732
Limiting indices	$-16 \le h \le 16$
	$-17 \le k \le 1$
	$-23 \le l \le 23$
Data/Restraints/Parameters	13394 / 18 / 1025
GOF on F_2	1.687
R1a	0.1231
wR2b	0.3528
R1	0.1440
wR2	0.3865

[a] $R_1 = \sum||F_o| - |F_c|| / \sum|F_o|$; [b] $wR_2 = [\sum[w (F_o^2 - F_c^2)^2] / \sum[w (F_o^2)^2]]^{1/2}$.

Table S2. Crystal data and structure refinement parameters of **Cu-atda**

Identification code	**Cu-atda**
Empirical formula	$C_{16}H_{12}CuN_4O_5$
CCDC	2101553
Formula mass	403.84
Crystal system	Monoclinic
Space group	P2(1)/m
a (Å)	10.1215(5)
b (Å)	20.6659(11)
c (Å)	10.3207(7)
α (˚)	90.00
β (˚)	93.249(2)
γ (˚)	90.00
V (Å3)	2155.3(2)
Z	4
Dc/(Mg m^{-3})	1.245
μ (Mo Kα)/mm^{-1}	1.042
F(000)	848
θ range (°)	2.209 – 30.500
Limiting indices	–13≤ h ≤ 14
	–29 ≤ k ≤ 28
	–11≤ l ≤ 14
Data/Restraints/Parameters	6693 / 0 / 217
GOF on F2	0.840
R1a	0.0427
wR2b	0.1221
R1	0.0595
wR2	0.1354

[a] $R_1 = \sum||F_o| - |F_c||/\sum|F_o|$; [b] $wR_2 = [\sum[w(F_o^2 - F_c^2)^2] / \sum[w(F_o^2)^2]]^{1/2}$.

Table S3. Selected bond lengths (Å) and bond angles (°) for **Cu-cboa**

Cu-cboa			
Cu(1)-N(10)	1.982(6)	Cu(1)-N(11)	2.034(7)
Cu(1)-N(15)	1.990(6)	Cu(1)-N(3)	2.045(5)
Cu(2)-O(15)	1.967(3)	Cu(2)-O(12)#1	1.969(3)
Cu(2)-O(18)	1.972(4)	Cu(2)-O(16)	1.980(4)
Cu(3)-O(24)	1.971(4)	Cu(3)-O(13)	1.972(3)
Cu(3)-O(14)	1.981(3)	Cu(3)-O(20)#2	1.994(3)
Cu(3)-N(12)	2.210(5)	Cu(4)-O(21)	1.938(4)
Cu(4)-O(22)	1.944(4)	Cu(4)-O(25)#1	1.948(3)
Cu(4)-O(10)	1.964(3)	Cu(4)-Cl(1)	2.4612(7)
Cu(5)-O(23)#2	1.949(3)	Cu(5)-O(17)	1.950(3)
Cu(5)-O(5)	1.953(4)	Cu(5)-O(19)	1.956(4)
Cu(5)-Cl(2)	2.4631(6)		
N(10)-Cu(1)-N(15)	109.2(3)	N(15)-Cu(1)-N(11)	100.4(3)
N(10)-Cu(1)-N(11)	117.8(3)	N(10)-Cu(1)-N(3)	126.0(2)
N(15)-Cu(1)-N(3)	103.7(3)	N(11)-Cu(1)-N(3)	96.0(2)
O(15)-Cu(2)-O(12)#1	171.47(15)	O(15)-Cu(2)-O(18)	90.26(16)
O(12)#1-Cu(2)-O(18)	88.38(16)	O(15)-Cu(2)-O(16)	87.87(15)
O(12)#1-Cu(2)-O(16)	91.69(16)	O(18)-Cu(2)-O(16)	167.79(14)
O(15)-Cu(2)-N(1)	99.31(15)	O(12)#1-Cu(2)-N(1)	89.11(15)
O(18)-Cu(2)-N(1)	89.89(15)	O(16)-Cu(2)-N(1)	102.32(15)
O(24)-Cu(3)-O(13)	87.55(15)	O(13)-Cu(3)-O(14)	89.16(15)
O(24)-Cu(3)-O(14)	168.58(14)	O(24)-Cu(3)-O(20)#2	89.39(15)
O(13)-Cu(3)-O(20)#2	167.19(14)	O(14)-Cu(3)-O(20)#2	91.43(15)
O(24)-Cu(3)-N(12)	99.99(18)	O(13)-Cu(3)-N(12)	103.61(18)
O(14)-Cu(3)-N(12)	91.40(18)	O(20)#2-Cu(3)-N(12)	89.17(18)
O(21)-Cu(4)-O(25)#1	89.43(18)	O(21)-Cu(4)-O(22)	166.68(15)
O(22)-Cu(4)-O(25)#1	89.80(19)	O(21)-Cu(4)-O(10)	88.92(18)
O(22)-Cu(4)-O(10)	88.01(19)	O(25)#1-Cu(4)-O(10)	163.29(15)
O(21)-Cu(4)-Cl(1)	94.94(11)	O(22)-Cu(4)-Cl(1)	98.33(11)
O(25)#1-Cu(4)-Cl(1)	97.81(11)	O(10)-Cu(4)-Cl(1)	98.90(11)
O(23)#2-Cu(5)-O(17)	166.15(15)	O(23)#2-Cu(5)-O(5)	89.33(18)
O(17)-Cu(5)-O(5)	87.59(18)	O(23)#2-Cu(5)-O(19)	89.81(17)
O(17)-Cu(5)-O(19)	89.58(18)	O(5)-Cu(5)-O(19)	164.54(15)
O(23)#2-Cu(5)-Cl(2)	96.02(11)	O(17)-Cu(5)-Cl(2)	97.81(11)
O(5)-Cu(5)-Cl(2)	100.17(11)	O(19)-Cu(5)-Cl(2)	95.27(10)
N(7)-Cu(1)-Cl(1)	90.50(6)	Cl(2)-Cu(1)-Cl(1)	150.07(4)

Table S4. Selected bond lengths (Å) and bond angles (°) for **Cu-atda**

Cu-atda			
Cu(1)-O(3)	1.9556(13)	Cu(1)-O(1)	1.9634(13)
Cu(1)-O(2)	1.9595(13)	Cu(1)-O(4)	1.9739(12)
Cu(1)-O(5)	2.1733(13)		
O(3)-Cu(1)-O(2)	87.97(6)	O(3)-Cu(1)-O(4)	168.15(5)
O(3)-Cu(1)-O(1)	87.99(6)	O(2)-Cu(1)-O(4)	89.29(6)
O(2)-Cu(1)-O(1)	168.02(5)	O(1)-Cu(1)-O(4)	92.38(6)
O(3)-Cu(1)-O(5)	96.44(5)	O(2)-Cu(1)-O(5)	100.55(6)
O(1)-Cu(1)-O(5)	91.10(6)	O(4)-Cu(1)-O(5)	95.39(5)

Table S5. The LOD of FQ of other sensors.

sensors	LOD	Ref.
9A/Cu-atda@Eu^{3+}/SA	48 nM	This work
MA-IPA@SA	0.114 ppm	**1**
SAW	10^{-6} M	**2**
Eu@ZIF-90–PA	0.24 ppm	**3**
recombinant antibody	0.6 μg L^{-1}	**4**
SH-SAW	1 μM	**5**
UHPLC–FL	5.0 μg L^{-1}	**6**

SAW: surface acoustic wave sensor
SH-SAW: shear horizontal surface acoustic wave sensor
UHPLC–FL :Ultra-high performance liquid chromatography coupled to fluorescence detection

1. N. Ktari, N. Fourati, C. Zerrouki, M. Ruan, D. Nassoko, M. Seydou, N. Yaakoubi, M. M. Chehimi and R. Kalfat, *Procedia Engineering*, 2015, **120**, 998-1002.
2. X. Xu, J. Wang and B. Yan, *Adv. Fun. Mater.*, 2021, DOI: 10.1002/adfm.202103321, 1-10.
3. S. Li, Y. Li and B. Yan, *CrystEngComm*, 2021, **23**, 5345-5352.
4. J. Leivo, U. Lamminmaki, T. Lovgren and M. Vehniainen, *J. Agric. Food. Chem.*, 2013, **61**, 11981-11985.
5. N. Ktari, N. Fourati, C. Zerrouki, M. Ruan, M. Seydou, F. Barbaut, F. Nal, N. Yaakou, M. M. Chehimi and R. Kalfat, *RSC Adv.*, 2015, **5**, 88666–88674.
6. N. Arroyo-Manzanares, J. F. Huertas-P, M. L.-A. erez, L. Gamiz-Gracia, A. M. Garc and ıa-Campana, *Anal. Methods*, 2015, **7**, 253–259.